

## Ultrasonic Spectroscopy to Characterize Flaws, Porosity and Adhesive Bonds

Laszlo Adler

Taine McDougal Professor Emeritus

Ohio State University/Adler Consultants Inc.

Clearwater, Florida, USA

### ABSTRACT

Ultrasonic Spectroscopy is the study of ultrasonic waves resolved into their Fourier frequency components. Since most material properties manifest themselves as amplitude and phase changes in ultrasonic waves used to interrogate a specimen, ultrasonic spectroscopy is used in many applications of Nondestructive Evaluation. In this presentation three methods developed by the author to apply ultrasonic spectroscopy in NDE will be discussed.

Flaw characterization. refers to the determination of size, orientation, and composition of discontinuities in solid materials. Multifrequency (broad band) ultrasonic wave interaction with artificial and real defects measurements and subsequent theoretical analysis using diffraction of elastic waves provides these material discontinuities' characteristics.

Gas porosity assessment. Measuring pore size and volume fraction from the spectrum of attenuation coefficient will be discussed. Theoretical analysis is based on the attenuation due to independent scatterer of spherical voids. The model prediction of the scattering of ultrasonic waves from porosities is in good agreement with measured values in aluminum casts.

Evaluation of Adhesive Layers. Linear and nonlinear spectroscopic systems were developed to determine both adhesive and cohesive properties of thin bonded layers using multi transducer spectroscopy. Scattered longitudinal and transverse waves spectra is used in this method. The method was further enhanced by combining with a low frequency dynamic load acting as a nonlinear (parametric) enhancement. Ultrasonic measurements are in good agreement with actual layer properties.

Keywords: ultrasonics, spectroscopy, nondestructive evaluation

### 1. INTRODUCTION

Ultrasonic spectroscopy is the study of ultrasonic waves resolved into Fourier frequency components. The schematic1 of a multipurpose ultrasonic system is shown on figure 1.

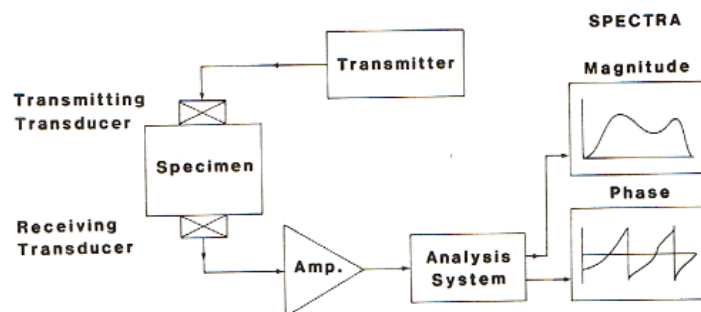


Figure1 - Generalized ultrasonic spectroscopy system

In this paper several applications of ultrasonic spectroscopy in NDE will be discussed.

## 2. FLAW CHARACTERIZATION

The first experimental system was developed by Gericke<sup>2</sup> in using a contact method and by Whaley and Adler<sup>3</sup> immersion method. Both these methods quickly established the variation of frequency spectrum with flaw characteristics.

### 2.1 Reflection experiments with metal rods

A flaw in metal may be simulated by using the end of a metal rod in water. In both cases the acoustic impedances are significantly different from each other thus causing a large reflected signal. Ultrasonic pulses were generated in water with a broadband transducer and received and analyzed after reflecting from the ends of sample brass rods. The end of the rods was machined flat and smooth with diameter ranging from 0.281 to 0.031 inches (7.1 to 079 mm). The positioning and the rotation of the sample is achieved by a very precise Turntable, see, fig. 1. The transducer, nominally 2.25 MHz and .75 inch in diameter, was used with 6 inch water paths.

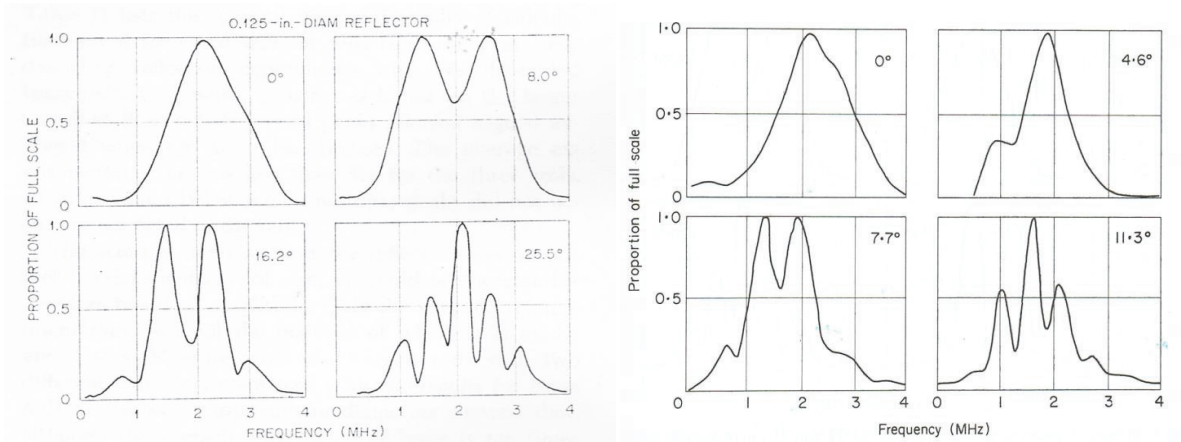


Figure 2 - Variations in ultrasonic spectra at various angles of incidence for the 0.125 in. and .281 in diameter brass reflector.

Figure 2 presents the representative data obtained in these tests showing the angular and size dependence of the shape of the frequency spectrum of a pulse reflected from brass rod. The shapes of the spectrum at normal incidence for all rods were essentially the same as the reflected spectrum from a large plate normal to the transducer axis. The principal frequency is shifted in position as the angle of incidence changed.

## 2.2 Suggested model for the reflected spectra from discontinuities

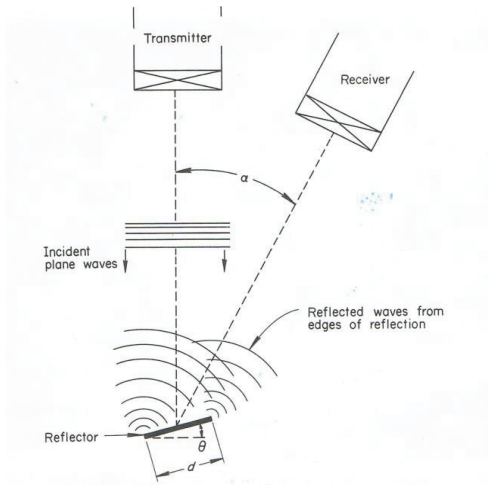


Figure 3 - Schematic diagram of the interference model

In this model it is assumed that when a multifrequency wavefront is generated by a circular transducer it becomes a plane wave in the far field. A circular reflector with diameter  $d$  is placed in the far field of the transducer and the axes of the transducer and reflector are oriented by an angle  $\theta$  with respect to each other. It was assumed that the incident plane wave breaks up into three parts when it is reflected: a specular reflection and two wavelets originating from the edges of the reflector. The wavelets are coherent sources that interfere at the face of the transducer. Because these wavelets contain a broad range of frequencies, the condition for constructive interference will always be satisfied for some frequencies. From geometrical considerations, after some simplification, one obtains a formula for the difference of two consecutive frequency maxima

$$\Delta f = v/[d \sin \theta + d \sin(\theta + \alpha)] \quad (1)$$

where  $v$  is the velocity of the sound. In order to obtain both size and orientation of the reflector a second equation like (1) is needed, which can be obtained by carrying out measurement for  $\Delta f$  say  $\Delta f'$  and position  $\alpha'$ . Then

$$\Delta f' = v/[d \sin \theta + d \sin(\theta + \alpha')] \quad (2)$$

from (1) and (2) both  $d$  and  $\theta$  can be evaluated.

## 2.3 Flaws Embedded in Solids

The determination of size for variously shaped reflectors was applied to randomly shaped shims shown on figure 4. Notice that in addition to circular, elliptical and rectangular reflectors there are irregular shaped reflectors (see numbers 4, 5 and 8 in figure 29). By aligning the transmitter-receiver plane at various orientations, several dimensions of the reflectors can be determined using equations 35 and 36.

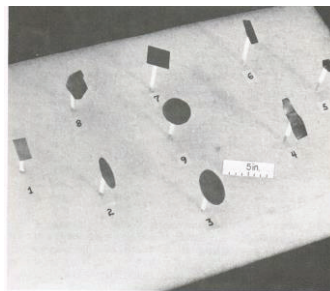


Figure 4 - Photograph of various reflectors used in the experiment

In table 1, the actual and measured values of the various dimensions are shown for all the reflectors (simulating flaws) used. The agreement between actual values and measured values of the reflectors is good –within 10-15%.

Flaw type	Dimensions	Flaw size in inches*	
		Actual	Measured
1. Rectangular	Small side	0.25	0.23
	Long side	0.43	0.48
2. Ellipse	Small diameter	0.2	0.25
	Long diameter	0.55	0.53
3. Ellipse	Small diameter	0.46	0.41
	Long diameter	0.85	0.75
4. Irregular	Smallest	0.26	0.29
	Largest	0.81	0.74
5. Irregular	Smallest	0.23	0.23
	Largest	0.29	0.26
6. Rectangular	Small side	0.19	0.29
	Long side	0.63	0.60
7. Square	Side	0.48	0.45
8. Irregular	Smallest	0.42	0.37
	Largest	0.69	0.62
9. Circle	Diameter	0.52	0.53

Table 1 – Comparison of Actual and Measured Sizes for Simulated “Real Flaws”

Additional samples used to simulate defects in solids. Two cylinders of titanium alloy were machined and their bases diffusion bonded together in such way that the final longer cylinder contained a cavity in the center. On figure 5 the geometry of the simulated defects is shown.

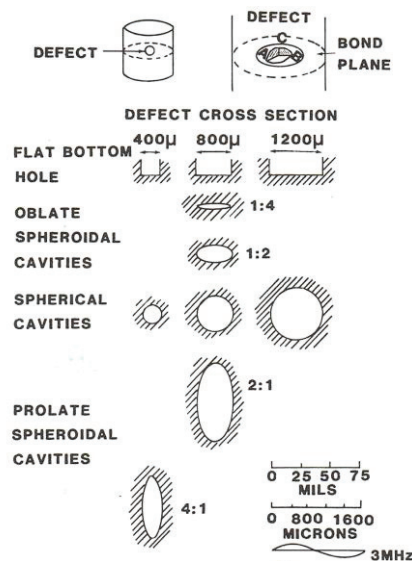


Figure 5 - Simulated defects of various sizes and shapes in a diffusion bonded titanium disk.

A schematic of the experimental setup used in our scattering measurements is shown on figure 6. For an incident longitudinal wave both the scattered longitudinal and the scattered shear waves are measured separately as shown on figure 6.

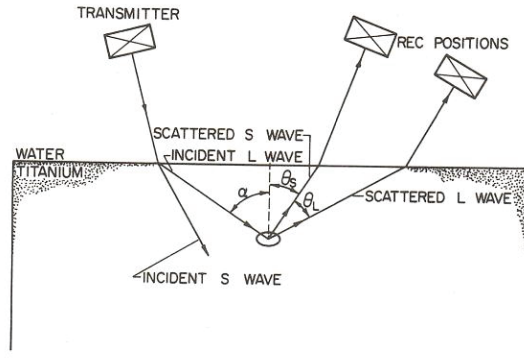


Figure 6 - Experimental technique for the study of scattering from defects in immersed specimen.

Experimental and theoretical amplitude spectra of scattered waves from 2500x1250 $\mu$ m elliptical cracks are shown in figure 7.

The favorable results from these model experiments indicate that the amplitude spectra of elastic wave scattering from well-defined geometrical flaws can be predicted by theoretical analysis, of Jan Adler and Achenbach<sup>4</sup>, in metals.

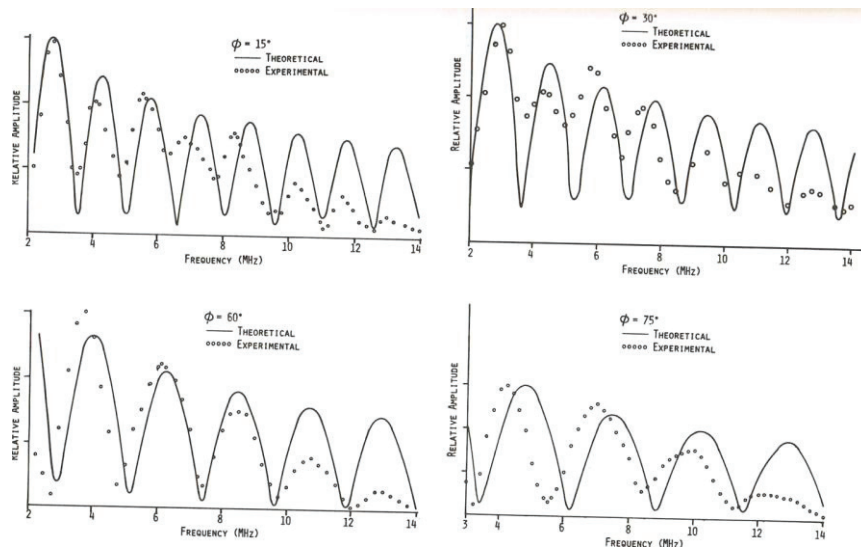


Figure 7 - Amplitude spectra of scattered longitudinal waves from a 2500x1250 $\mu$ m elliptical crack in titanium along different azimuthal directions, polar angle is 60<sup>o</sup>

### 3. POROSITY ASSESSMENT IN ALUMINUM CASTS

Aluminum casts are used in many parts of airplanes and extensive porosity can cause catastrophic failure. The frequency dependence of ultrasonic attenuation measurement proved to provide both pore concentration and average pore size. The procedure of the measurement is shown schematically in figure 8 where the front surface, back surface and deconvolved spectrum are shown respectively.

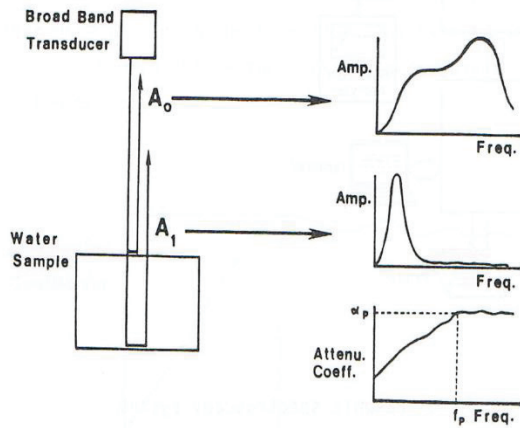


Figure 8 - Ultrasonic spectra from an aluminum block with porosity immersed in water.

Theoretical consideration<sup>5</sup> from the turning point  $f_p$  using single spherical scatterer provided two parameters for the aluminum sample.

$$R = (v/2\pi)(1/f_p) \quad (3) \text{ and}$$

$$C = (V/2\pi K)(\alpha_p/f_p) \quad (4)$$

where  $R$  is the average pore radius,  $C$  is the pore concentration  $v$  is the velocity of the ultrasound in the sample and  $K$  is a constant dependent on the material.

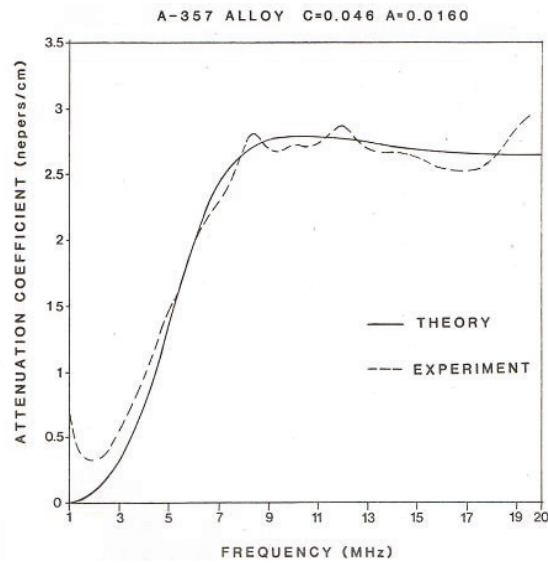


Figure 9 - Comparison of theoretical and experimental result for the frequency dependent attenuation coefficient in an aluminum cast alloy.

Using equation 3 and 4 the ultrasonic results favorably compared to actual values obtained from density measurement for 11 samples as shown

Sample	Attenuation Coefficient (NP/cm)	Frequency (NHZ)	$K_0$ (1/cm)	Pore Radius ( $\mu\text{m}$ )	Porosity	
					Exp.	Density
Cast A1 013	.39	15	142	70	.24	---
Cast A1 1010	.22	12	114	87	.17	0
Cast A1 1210	.20	8	76	131	.23	.22
Cast A1 1410H	1.02	13	123	80	.74	1.3
Cast A1 1410L	.20	10	95	195	.19	1.3
Cast A1 1510	1.12	9	85	116	1.18	2.18
Cast A1 1810	1.00	10	95	105	.95	.9
Cast A1 1820	1.25	12	114	87	.99	1.05
Cast A1 1830	1.20	11.5	109	91	.99	1.20
Cast A1 1850	1.00	11	104	95	.86	1.08
Cast A1 1920	2.85	8	76	131	3.4	4.6

Table 2 - Summary of ultrasonic results of cast samples

#### 4. ADHESIVE LAYER EVALUATION

In the Angle beam Ultrasonic Spectroscopy<sup>6</sup> approach obliquely and normally incident ultrasonic beam are combined. The two angle measurements allow decoupling the effects of the bond line thickness. To do this we developed a transducer head schematically shown in figure 10-. The head accommodates transducers for the normal and oblique measurements. The ultrasonic wave excited by the transducer is reflected from the interface toward a reflector and returns back to the transducer. The procedure used to scan the quality of the thin adhesive layer embedded between two composite plates is twofold. At each point of the scan, the normal and angle beam time domain signals reflected from the layer are recorded. Then they are analyzed in the Fourier domain and processed using our algorithms to obtain the quality of the bond line.

The time signals are recorded using the transducer head. The transducer head is moved over the sample from point to point and each acquisition is recorded. The collected time domain signals are stored in the form of a 2-D array corresponding to the sampled scan area.

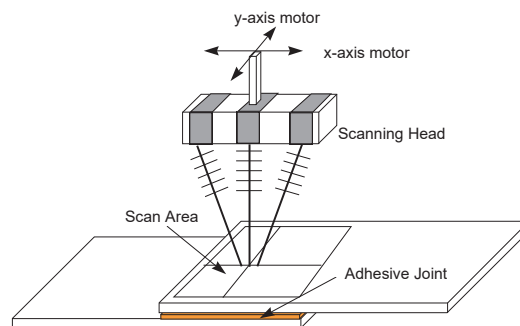


Figure 10 - Transducer head

After acquisition of the time signals, the second step is analysis in the Fourier domain of these signals to get the relevant parameters for the layer properties determination. The following procedure is applied for each point:

- Gating of the useful part of the time domain signal
- Computation of the Fast Fourier Transform
- Gating of the useful part of the frequency domain signal
- Determination of the resonance position (in Mhz) and width.
- Model-based computation of the layer properties at the corresponding point.

The final result (bond line quality reconstruction for every scanned points) is displayed as a bond line quality image in color level shown on figure 11 together with their relation to bond strength.

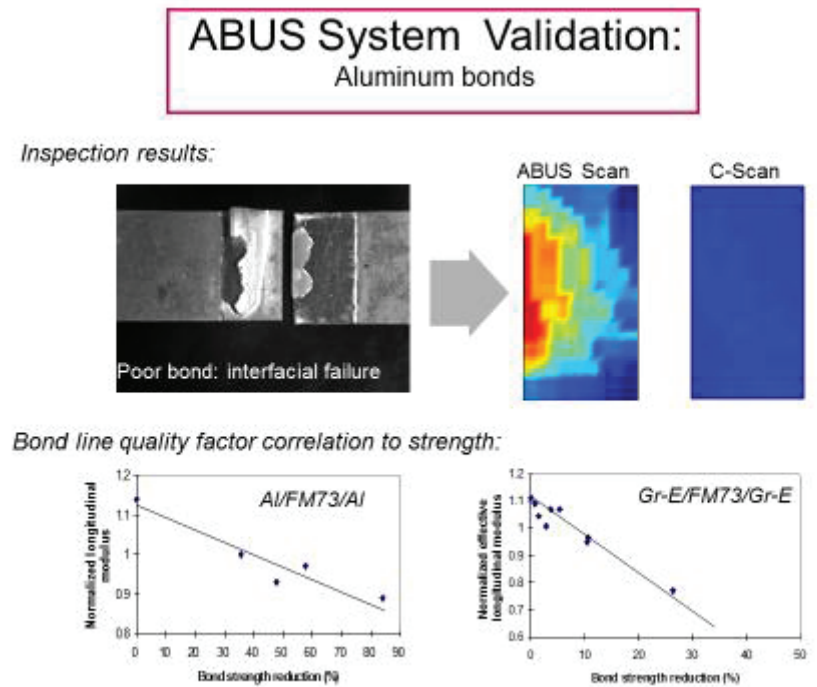


Figure 11 Experimental results.

While the ABUS scan clearly displays the fracture no information is obtained by C scan.

**This work was partially supported by a grant from the Emeritus Academy OSU.**

## REFERENCES

1. Fitting, D. E. and Adler L.: Ultrasonic Spectral Analysis for Nondestructive Evaluation, Plenum Press, New York, 1981.
  2. Gericke, O .R: Determination of the Geometry of Hidden Defects by Ultrasonic Pulse Analysis Testing, Journal of the Acoustical Society of America, 35 (1963), 364..
  3. Whaley, H.L. and Adler, L.: Flaw Characterization by Ultrasonic Frequency Analysis, Materials Evaluation, 29 (1971)
  4. Adler. L. and Achenbach J.D.: Elastic Wave Diffraction by Elliptical Cracks: Theory and Experiment Journal of Nondestructive Evaluation 1 (1980)
  5. Adler. L , Rose J. H. and Mobley C.: Ultrasonic Method to Determine Gas Porosity in Aluminum Alloy Castings: Theory and Experiment. Journal of Applied Physics 55(19860)
  6. Rokhlin. S., Wang. I. Xie. B. Yakovlev. V. and Adler. L. Modulated Angle Beam Ultrasonic Spectroscopy for Evaluation of Imperfect Interfaces and Adhesive Bonds ) Ultrasonics 42 (2004)
- This work was partially supported by